Bioorg. Med. Chem. Lett. 47 (2021) 128208

Contents lists available at ScienceDirect

Bioorganic & Medicinal Chemistry Letters

journal homepage: www.elsevier.com/locate/bmcl

Synthesis of NVS-BPTF-1 and evaluation of its biological activity

Léa Mélin [a], Cyrus Calosing [b], Olesya A. Kharenko [b], Henrik C. Hansen [b], Alexandre Gagnon [a,*]

[a] Département de chimie, Université du Québec à Montréal, C.P. 8888, Succ. Centre-Ville, Montréal, Québec H3C 3P8, Canada
[b] Zenith Epigenetics Ltd, Suite 300, 4820 Richard Road SW, Calgary, AB T3E 6L1, Canada

ARTICLE INFO

Keywords:
NVS-BPTF-1
BPTF
NURF
Synthesis

ABSTRACT

BPTF (bromodomain and PHD finger containing transcription factor) is a multidomain protein that plays essential roles in transcriptional regulation, *T*-cell homeostasis and stem cell pluripotency. As part of the chromatin remodeling complex hNURF (nucleosome remodeling factor), BPTF epigenetic reader subunits are particularly important for BPTF cellular function. Here we report the synthesis of NVS-BPTF-1, a previously reported highly potent and selective BPTF-bromodomain inhibitor. Evaluation of the impact of the inhibition of BPTF-bromodomain using NVS-BPTF-1 on selected proteins involved in the antigen processing pathway revealed that exclusively targeting BPTF-bromodomain is insufficient to observe an increase of PSMB8, PSMB9, TAP1 and TAP2 proteins.

Gene expression is highly regulated by chromatin topology. Even in the euchromatin state, transcription factors can hardly access the *cis*-sequences of DNA and usually require the combined action of both epigenetic enzymes and chromatin remodelers beforehand. Covalent modifications of histone tails, increased exposition of naked DNA or alteration of nucleosomes organization in a promoter region can strongly impact gene expression and, ultimately, cell phenotypes.[1]

NURF (nucleosome remodeling factor) is one of the conserved ATP-dependent chromatin remodeling factors belonging to the ISWI family. Rather than binding to naked DNA or histones, NURF preferentially interacts with nucleosomes through the positively charged *N*-terminal histone tails[2] and catalyzes nucleosome sliding.[3] By doing so, NURF is able to assist the binding of transcription factors and is therefore key for gene activation initiation.[4] Human NURF (hNURF) is composed of three subunits: the conserved ISWI ATPase core SNF2L, BPTF (bromodomain and PHD finger containing transcription factor, also known as FALZ for fetal alzheimer antigen) and RbAP48/46 (retinoblastoma associated proteins 46 and 48), two mammalian orthologs of Drosophila NURF301 and NURF55, respectively.[5]

BPTF, the largest and most essential component of the hNURF complex, is critical for transcriptional regulation during embryogenesis.[6,7] Outside of this specific developmental stage, BPTF maintains chromatin accessibility, allowing stem cell pluripotency,[8] *T*-cell homeostasis and function,[9] and transcriptional regulation.[10] In order to do so, BPTF harbors multiple motifs characteristic of transcriptional coactivators: one non-BET (bromodomain and extra-terminal domain) bromodomain, two PHD domains and a glutamine-rich acidic domain.[11] These epigenetic readers are particularly important for BPTF cellular function as they serve as recognition units for acetylated or methylated lysine residues. It has therefore been demonstrated that BPTF binds to acetylated H3 and H4 histone tails via its bromodomain and to H3K4Me3 via its second PHD finger.[12]

As lysine acetylation of histone tails is one of the most dynamic post-translation modification associated with chromatin accessibility and increased gene expression,[13] mutation and overexpression of bromodomain containing proteins (BCPs) have been associated with many diseases, such as cancer, inflammation or neurological disorders.[14] In particular, aberrant expression of BPTF has been implicated in the development and progression of multiple types of cancer, including colorectal cancer,[15] lung adenocarcinomas,[16] melanoma,[17] and neuroblastomas.[18] Slowly emerging as a potential target for novel anti-cancer drugs because of its required recruitment for c-MYC activation,[19,20] it is interesting to note that BPTF knockdowns enhance $CD8^+$ *T*-cell and NK-cells mediated antitumor immunity,[21,22] therefore also highlighting BPTF as a potential target for the development of immunotherapies.

Despite BPTF biological pertinence in cancer and the fact that inhibiting the bromodomain of BCPs has been successful in the past for treating BCPs-related diseases (as illustrated by the numerous BET inhibitors currently in clinical trials), only few chemical probes targeting BPTF-bromodomain have been developed (Fig. 1). AU1, the first small molecule showing some selectivity for BPTF, was reported in 2015.[23] Discovered during an ^{19}F NMR dual screening against BPTF and BRD4,

* Corresponding author.
E-mail address: gagnon.alexandre@uqam.ca (A. Gagnon).

https://doi.org/10.1016/j.bmcl.2021.128208
Received 29 April 2021; Received in revised form 9 June 2021; Accepted 13 June 2021
Available online 16 June 2021

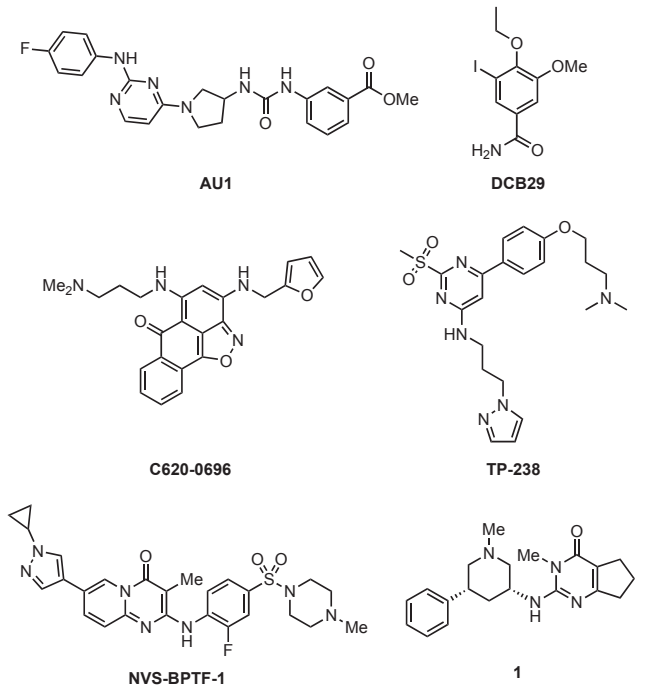

Fig. 1. Reported BPTF inhibitors.

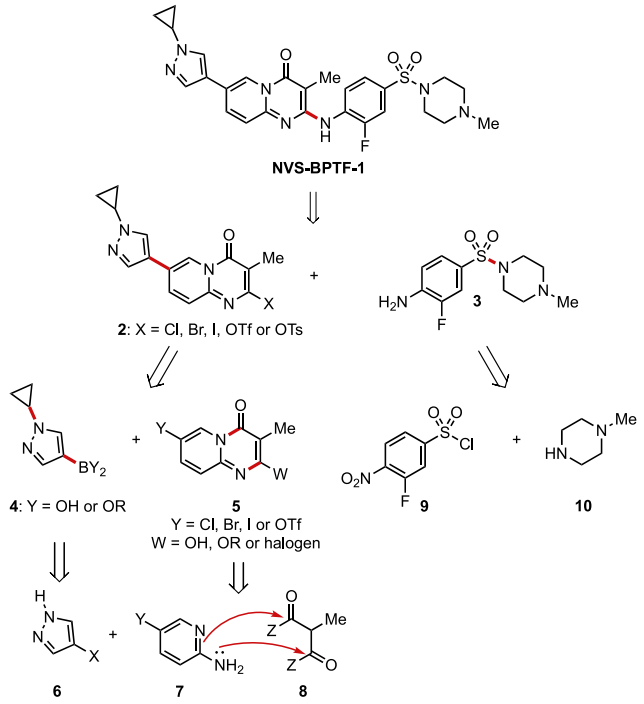

Scheme 1. Retrosynthetic analysis of NVS-BPTF-1.

AU1 displays a K_d value of 2.8 μM for BPTF as determined by isothermal titration calorimetry (ITC), while no binding against BRD4 was observed. In 2019, DCB29, a dialkoxy iodo benzamide derivative, was developed through structure-based virtual screening as a selective BPTF-bromodomain inhibitor with an IC_{50} value of 13.2 μM, obtained by homogenous time-resolved fluorescence resonance energy transfer (HTRF) assays.[24] The same year, compound C620-0696 was reported with a K_d value of 35.5 μM against BPTF as assessed by a biolayer interferometry (BLI) assay. C620-0696 exhibits cytotoxicity to BPTF overexpression in non-small-cell lung cancer (NSCLC) cell lines and also inhibits the binding between the BPTF bromodomain and H4K16Ac, which leads to repression of c-MYC transcription activation.[25]

Finally, the SGC, in collaboration with Takeda, reported on their website TP-238, the first chemical probe with low nanomolar potency against BPTF bromodomain. However, TP-238 inhibited both CECR2 and BPTF in an AlphaScreen assay with IC_{50} values of 30 nM and 350 nM, respectively.[26] This lack of selectivity was countered with the release of NVS-BPTF-1. Produced through a collaboration between the SGC and Novartis, NVS-BPTF-1 is the first highly potent, selective and cell active chemical probe for BPTF-bromodomain. NVS-BPTF-1 gave an IC_{50} value of 56 nM in an AlphaScreen assay and a K_d value of 71 nM in a BLI assay.[27] A DSF screen and a BROMOscan revealed no significant interaction with a panel of other human bromodomains. In HEK293 cells, NVS-BPTF-1 showed on-target activity with an IC_{50} of 16 nM, as measured by a nanoBRET assay. While writing this manuscript, compound **1** was published as a new BPTF-bromodomain inhibitor with a K_d value of 428 nM for BPTF as determined by ITC. Compound **1** down-regulated both c-MYC and BPTF expression in A549 cells.[28]

Even though NVS-BPTF-1 is currently the most potent and selective chemical probe against BPTF, to the best of our knowledge, its synthesis has not been reported yet. We would like to disclose herein a rapid and modular chemical route to access this tool compound. Preliminary evaluation of the biological activity of NVS-BPTF-1 is also described.

The retrosynthetic analysis of NVS-BPTF-1 invited a disconnection on the central aniline function, leading to the left-hand side pyridopyrimidinone synthon **2** and the right-hand side 1-((3-fluoro-4-aminophenyl)sulfonyl)-4-methylpiperazine fragment **3** (Scheme 1). We envisioned that the presence of a suitable leaving group X on **2** such as an halide, a triflate or a tosylate could allow an S_NAr transformation or a metal-catalyzed *N*-arylation reaction with **3**. Although complications could arise from the anticipated low nucleophilicity of aniline **3**, we hypothesized that this approach would have a higher chance of success than the complementary C—N disconnection that would require the preparation of an intriguing and poorly-characterized amino-pyrimidinone version of **2** (i.e. X = NH_2). Left-hand side fragment **2** could then be prepared by a palladium-catalyzed cross-coupling reaction between an *N*-cyclopropylboron species **4**, either in the form of a boronic acid or ester, and a halo or triflyl pyridopyrimidinone core of type **5**. Should this cross-coupling be challenging, we assumed that the role of the partners could be inverted, that is, the boron function would be installed on **5**. The installation of the cyclopropyl unit on the pyrazole's NH would be performed through a copper-catalyzed *N*-cyclopropylation reaction on **6** via one of the numerous conditions involving boron or bismuth reagents. The boron would be installed on **6** via a lithium–halogen exchange reaction or a metal-catalyzed cross-coupling process. A search of the literature revealed a paucity of methods to form the densely functionalized central core **5**. It was our hope that this scaffold could be obtained by a condensation reaction between **7** and a properly activated malonic system **8**. Finally, the aniline portion **3** would be prepared from **9** and **10** through conventional sulfonamide bond construction and nitro reduction.

We first prepared aniline **3** by reacting 3-fluoro-4-nitrobenzenesulfonyl chloride **9** with 1-methylpiperazine **10**, followed by reduction of the nitro group in **11** under Béchamp's conditions (Scheme 2). Quick attempt at improving the yield of this transformation, for example by increasing the reaction time or the temperature, or pre-forming the sodium amide of **10** proved unsuccessful and therefore, we continued with the synthesis of the western portion of our target molecule.

Thus, we prepared the *N*-cyclopropyl-4-borylpyrazolyl synthon **4** (c.f. Scheme 1) by first installing the cyclopropyl moiety onto 1-cyclopropyl-4-iodo-1*H*-pyrazole **12** via a copper-catalyzed *N*-cyclopropylation reaction (Scheme 3). After testing various conditions, we found that this transformation could be efficiently accomplished using 2.0 equivalents of cyclopropylboronic acid in the presence of a stoichiometric amount of cupric acetate and a mixture of dimethylaminopyridine and pyridine in refluxing dioxane under an oxygen atmosphere.

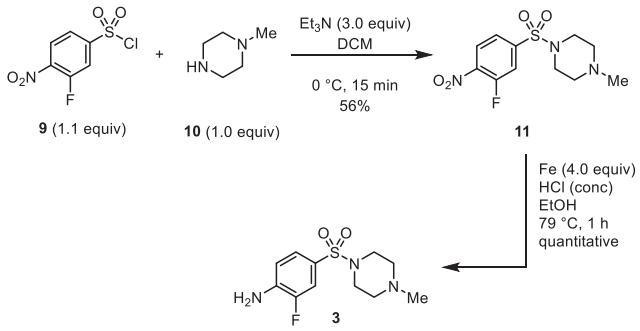

Scheme 2. Synthesis of aniline **3**.

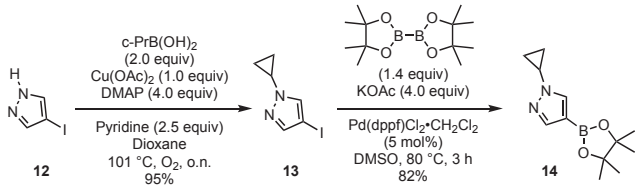

Scheme 3. Synthesis of 1-cyclopropyl-4-(4,4,5,5-tetramethyl-1,3,2-dioxaborolan-2-yl)-1*H*-pyrazole **14**.

Attempts at transforming the iodide in **13** into a boron functionality through a lithium–halogen exchange process followed by reaction with trimethylborate proved difficult. Consequently, iodide **13** was converted into the corresponding 1-cyclopropyl-4-(4,4,5,5-tetramethyl-1,3,2-dioxaborolan-2-yl)-1*H*-pyrazole **14** via a palladium-catalyzed cross-coupling reaction with bis(pinacolato)diboron. Rapid optimization of the reaction conditions led us to use [1,1′-bis(diphenyl-phosphino) ferrocene]-dichloropalladium(II) as the catalyst in combination with potassium acetate as the base and DMSO as the solvent.

We next turned our attention to the preparation of the pyridopyrimidinone scaffold **5** (c.f. Scheme 1). A quick search of the literature indicated a lack of methods to prepare compounds of this type with a methyl group in position 3. Attempts at directly coupling 5-bromoaminopyridine **15** with 2-methylmalonic dimethylester **16** under smooth or forcing conditions failed to deliver the desired condensation product **17**, but provided instead a mixture of the mono-condensation adduct **18** and its corresponding decarboxylation product **19** (Scheme 4a).

We hypothesized that a more reactive malonic system could potentially facilitate this apparently difficult condensation reaction. Thus, 2-methylmalonic acid **20** was preactivated with HATU in the presence of Hünig's base and then reacted with **15** (Scheme 4b). Again, product **17** could not be isolated using this approach, even when conducted under drastic conditions. Ultimately, the cyclization problem was solved by transforming 2-methylmalonic acid **21** into its corresponding bis (2,4,6-trichlorophenyl)ester derivative **23** through reaction with 2,4,6-trichlorophenol **22** in neat phosphorus oxychloride (Scheme 4c). Reacting **23** with 5-bromo-2-aminopyridine **15** in hot toluene over 2 h finally afforded the desired cyclized product **17** in 83% yield (Scheme 4c).

Direct reaction of *N*-cyclopropylpyrazolylboronic pinacol ester **14** with bromopyrimidinone **17** was then attempted with the aim of generating **24** (Scheme 5). After testing numerous conditions, we could not obtain the desired product and we thus opted to convert the OH (which might also exist in the tautomeric keto-form) into the corresponding chloride. This chloride would serve as a valuable handle for a subsequent S_NAr reaction with aniline **3**. In the event, **17** was converted into **25** through heating in a mixture of phosphoryl chloride and phosphorus pentachloride. Unfortunately, all attempts to realize the S_NAr reaction between **25** and **3** failed, even under harsh conditions. Thus, **25** was engaged in a cross-coupling reaction with **14** with the hope that this

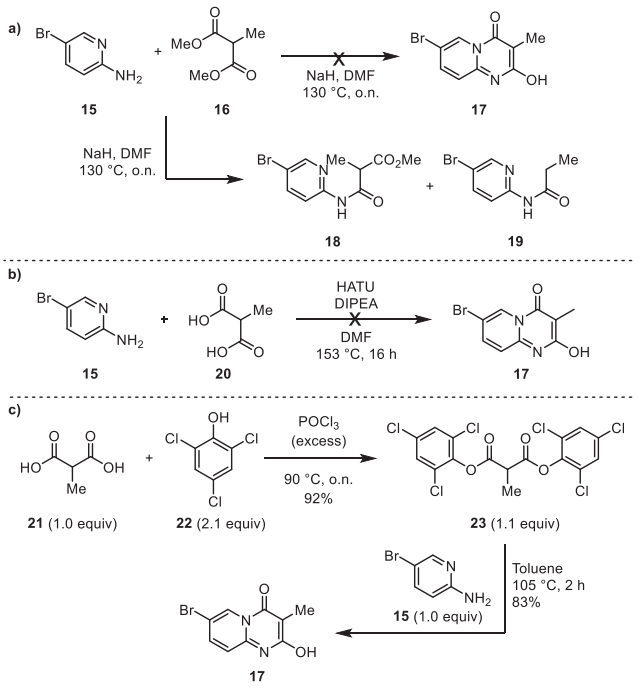

Scheme 4. Synthesis of the 7-bromo-2-hydroxy-3-methyl-4*H*-pyrido[1,2-*a*] pyrimidin-4-one core **17**.

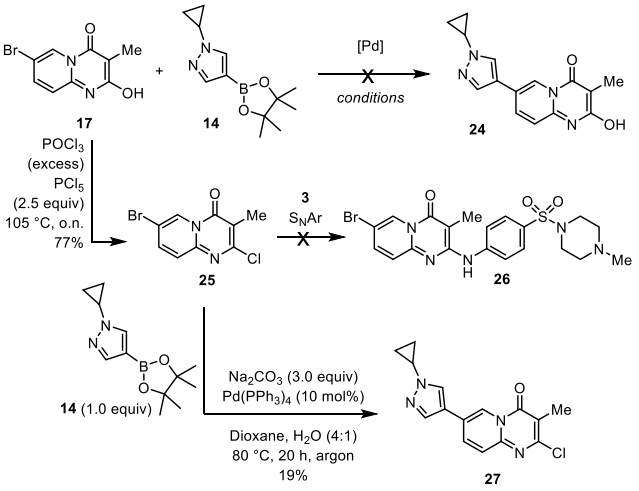

Scheme 5. Synthesis of pyridopyrimidinone **27**.

transformation would occur with some level of selectivity on the bromide over the chloride. Happily, this strategy delivered **27**, albeit in a moderate 19% yield. Since other catalysts or conditions failed to improve the efficiency of the process, we decided to continue with the union of **27** with **3**.

Attempts at coupling **3** and **27** through a S_NAr reaction under various conditions failed to provide the desired product NVS-BPTF-1. We assumed that the deactivation of the aniline **3** by the combined electron-withdrawing effects of the fluoride in *ortho* position and the sulfonamide in *para* were responsible (at least partially) for this lack of reactivity. Therefore, we turned our attention to a metal-catalyzed approach and found that key intermediates **3** and **27** could be coupled under Buchwald-Hartwig conditions using palladium(II) acetate, racemic BINAP in refluxing toluene in the presence of cesium carbonate, affording NVS-BPTF-1 in 56% yield with greater than 99% purity (Scheme 6).

The structure of synthetic NVS-BPTF-1 was confirmed through X-ray

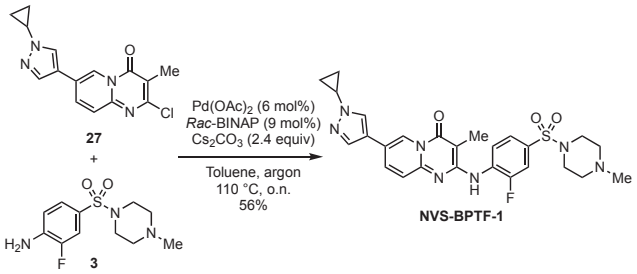

Scheme 6. Synthesis of NVS-BPTF-1 through Buchwald-Hartwig coupling between **27** and **3**.

diffraction analysis on crystals obtained from methylene chloride via the solvent diffusion technique (Fig. 2).

Mayes and collaborators have shown that depletion of BPTF in B16F10 models leads to upregulation of PSMB8 and PSMB9 which are part of the immunoproteasome, as well as TAP1 and TAP2 which belong to the transporter associated with antigen-processing complex.[21] They observed that this upregulation results in enhanced antigenicity and improved *T*-cell antitumor activity. With our resynthesized NVS-BPTF-1 in hand, we thus aimed to evaluate if inhibition of BPTF would result in a similar upregulation of these four specific proteins as in the knockdown model, thus allowing us to determine the potential therapeutic pertinence of BPTF-bromodomain in the context of immunotherapies for the treatment of cancer.

First, we confirmed the activity and the selective profile of NVS-BPTF-1 using both an AlphaScreen assay and a DSF thermal shift assay (differential scanning fluorimetry) against BPTF and BRD4(BD1) (Fig. 3). In the event, an IC_{50} of 30 nM and a ΔT_m of 5.7 °C were obtained, which are in good agreement with values presented online by the SGC (i.e. IC_{50} of 56 nM against BPTF in an AlphaScreen assay and ΔT_m of 6.16 °C).[27]

Since the selectivity of the probe was already assessed by the SGC via a DSF screen and a BROMOscan assay,[27] we then evaluated the effect of our compound on proliferation in various cancer cell lines. Contrary to AU1 and C620-0696, NVS-BPTF-1 did not affect the proliferation of B16F10 mouse melanoma cell lines (Fig. 4). While AU1 and C620-0696 are low micromolar inhibitors of the BPTF bromodomain, this difference could be attributed to off-target effects, previously reported in the literature.[29] In a similar fashion, NVS-BPTF-1 did not inhibit the proliferation of multiple human cancer cell lines (Fig. S1), while siRNA knockdowns of BPTF were previously reported as reducing proliferation of various cancer cell lines.[16,30,31]

Previous reports revealed that interferon gamma (IFNγ)[32] and shRNA knockdown of BPTF[21] can increase the amount of immunoproteasome proteins PSMB8 and PSMB9 and antigen transport proteins TAP1 and TAP2. Our results also indicate that BPTF siRNA knockdown

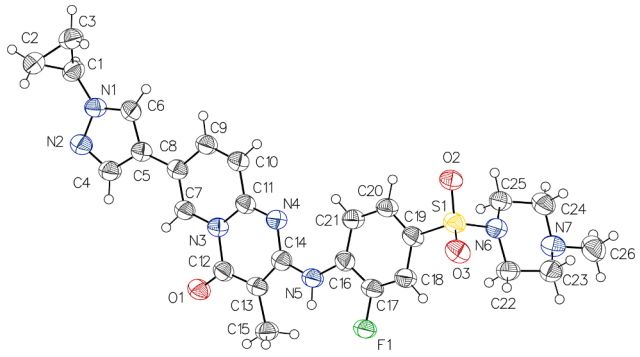

Fig. 2. Thermal atomic displacement ORTEP ellipsoid plot for NVS-BPTF-1 (CCDC number: 2080173). Ellipsoids are drawn at the 50% probability level and hydrogen atoms are shown as spheres of arbitrary size.

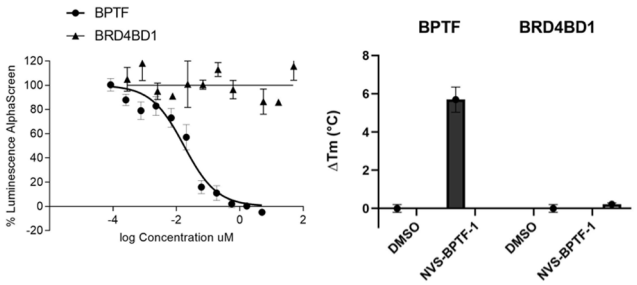

Fig. 3. a) AlphaScreen (IC_{50} = 30 nM; n = 4) and b) DSF (ΔT_m = 5.7 °C) assays using resynthesized NVS-BPTF-1 against BPTF and BRD4(BD1).

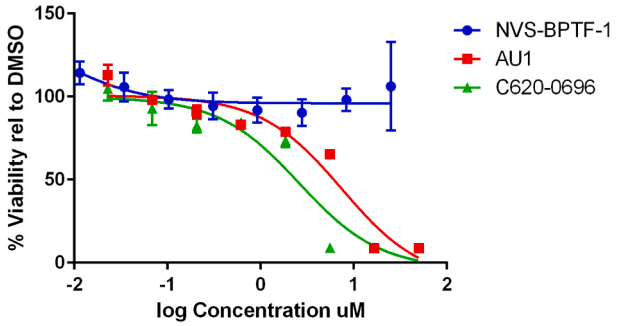

Fig. 4. Proliferation assay in B16F10 model.

can enhance the proteasome subunit beta type-9 protein (PSMB9) in B16F10 cells (Fig. S2). However, when NVS-BPTF-1 was used, this activation was not detected in B16F10 mouse melanoma cell lines (Fig. 5), nor in A549 (lung) or BT549 (breast) human cancer cell lines (Fig. S3).

Since NVS-BPTF-1 did not affect the level of PSMB8 and PSMB9 or TAP1 and TAP2, we hypothesized that targeting BPTF-bromodomain alone is not sufficient to observe any impact on the expression of these proteins.

In conclusion, a modular synthetic route was developed for NVS-BPTF-1, the first potent and selective inhibitor of BPTF bromodomain. Binding of resynthesized NVS-BPTF-1 to BPTF was confirmed using a DSF assay while inhibition was demonstrated using an AlphaScreen assay. No impact on B16F10 cell proliferation was observed upon exposure to NVS-BPTF-1. Contrary to BPTF knockdown models, inhibition of BPTF with NVS-BPTF-1 did not lead to increased levels of TAP1, TAP2, PSMB8 or PSMB9. These results suggest that only targeting BPTF-bromodomain might not be a viable strategy for the development of immunotherapies.

Declaration of Competing Interest

The authors declare that they have no known competing financial interests or personal relationships that could have appeared to influence

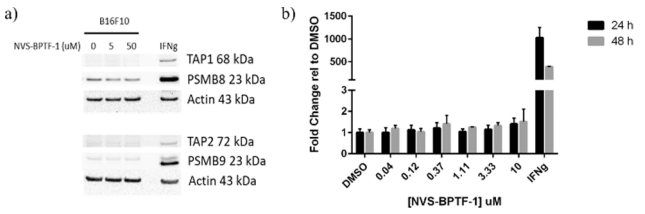

Fig. 5. Effects of NVS-BPTF-1 on PSMB8, PSMB9, TAP1 and TAP2. a) Western blot of B16F10 mouse melanoma cell lines treated with NVS-BPTF-1 or 20 ng/mL IFNg for 72 h; b) effects on PSMB9 mRNA in B16F10 mouse melanoma cell lines.

the work reported in this paper.

Acknowledgments

We would like to thank the Natural Sciences and Engineering Research Council of Canada (NSERC) and Zenith Epigenetics Ltd for a Collaborative Research and Development Grant. C.C., O.K., and H.H. are salaried employees of Zenith Epigenetics Ltd.

Appendix A. Supplementary data

Supplementary data to this article can be found online at https://doi.org/10.1016/j.bmcl.2021.128208.

References

1 Li B, Carey M, Workman JL. The role of chromatin during transcription. *Cell*. 2007;128(4):707–719. https://doi.org/10.1016/j.cell.2007.01.015.
2 Georgel PT, Tsukiyama T, Wu C. Role of histone tails in nucleosome remodeling by drosophila NURF. *EMBO J*. 1997;16(15):4717–4726. https://doi.org/10.1093/emboj/16.15.4717.
3 Hamiche A, Sandaltzopoulos R, Gdula DA, Wu C. ATP-dependent histone octamer sliding mediated by the chromatin remodeling complex NURF. *Cell*. 1999;97(7):833–842. https://doi.org/10.1016/s0092-8674(00)80796-5.
4 Mizuguchi G, Tsukiyama T, Wisniewski J, Wu C. Role of nucleosome remodeling factor NURF in transcriptional activation of chromatin. *Mol Cell*. 1997;1(1):141–150. https://doi.org/10.1016/S1097-2765(00)80015-5.
5 Barak O, Lazzaro MA, Lane WS, Speicher DW, Picketts DJ, Shiekhattar R. Isolation of Human NURF: a regulator of engrailed gene expression. *EMBO J*. 2003;22(22):6089–6100. https://doi.org/10.1093/emboj/cdg582.
6 Landry J, Sharov AA, Piao Y, et al. Essential role of chromatin remodeling protein Bptf in early mouse embryos and embryonic stem cells. *PLoS Genet*. 2008;4(10):e1000241. https://doi.org/10.1371/journal.pgen.1000241.
7 Goller T, Vauti F, Ramasamy S, Arnold H-H. Transcriptional regulator BPTF/FAC1 is essential for trophoblast differentiation during early mouse development. *Mol Cell Biol*. 2008;28(22):6819–6827. https://doi.org/10.1128/MCB.01058-08.
8 Frey WD, Chaudhry A, Slepicka PF, et al. BPTF maintains chromatin accessibility and the self-renewal capacity of mammary gland stem cells. *Stem Cell Rep*. 2017;9(1):23–31. https://doi.org/10.1016/j.stemcr.2017.04.031.
9 Wu B, Wang Y, Wang C, Wang GG, Wu J, Wan YY. BPTF is essential for T cell homeostasis and function. *J Immunol*. 2016;197(11):4325–4333. https://doi.org/10.4049/jimmunol.1600642.
10 Jordan-Sciutto KL, Dragich JM, Bowser R. DNA binding activity of the fetal Alz-50 clone 1 (FAC1) protein is enhanced by phosphorylation. *Biochem Biophys Res Commun*. 1999;260(3):785–789. https://doi.org/10.1006/bbrc.1999.0986.
11 Jones MH, Hamana N, Shimane M. Identification and characterization of BPTF, a novel bromodomain transcription factor. *Genomics*. 2000;63(1):35–39. https://doi.org/10.1006/geno.1999.6070.
12 Wysocka J, Swigut T, Xiao H, et al. A PHD finger of NURF couples histone H3 lysine 4 trimethylation with chromatin remodelling. *Nature*. 2006;442(7098):86–90. https://doi.org/10.1038/nature04815.
13 Shahbazian MD, Grunstein M. Functions of site-specific histone acetylation and deacetylation. *Annu Rev Biochem*. 2007;76(1):75–100. https://doi.org/10.1146/annurev.biochem.76.052705.162114.
14 Muller S, Filippakopoulos P, Knapp S. Bromodomains as therapeutic targets. *Expert Rev Mol Med*. 2011;13. https://doi.org/10.1017/S1462399411001992.
15 Xiao S, Liu L, Lu X, Long J, Zhou X, Fang M. The prognostic significance of bromodomain PHD-finger transcription factor in colorectal carcinoma and association with vimentin and E-cadherin. *J Cancer Res Clin Oncol*. 2015;141(8):1465–1474. https://doi.org/10.1007/s00432-015-1937-y.
16 Dai M, Lu J-J, Guo W, et al. BPTF promotes tumor growth and predicts poor prognosis in lung adenocarcinomas. *Oncotarget*. 2015;6(32):33878–33892.
17 Dar AA, Majid S, Bezrookove V, et al. BPTF transduces MITF-driven prosurvival signals in melanoma cells. *PNAS*. 2016;113(22):6254–6258. https://doi.org/10.1073/pnas.1606027113.
18 Buganim Y, Goldstein I, Lipson D, et al. A novel translocation breakpoint within the BPTF gene is associated with a pre-malignant phenotype. *PLoS ONE*. 2010;5(3):e9657. https://doi.org/10.1371/journal.pone.0009657.
19 Richart L, Carrillo-de Santa Pau E, Río-Machín A, et al. BPTF is required for C-MYC transcriptional activity and in vivo tumorigenesis. *Nat Commun*. 2016;7(1). https://doi.org/10.1038/ncomms10153.
20 Richart L, Real FX, Sanchez-Arevalo Lobo VJ. C-MYC partners with BPTF in human cancer. *Mol Cell Oncol*. 2016;3(3):e1152346. https://doi.org/10.1080/23723556.2016.1152346.
21 Mayes K, Alkhatib SG, Peterson K, et al. BPTF depletion enhances T-cell-mediated antitumor immunity. *Cancer Res*. 2016;76(21):6183–6192. https://doi.org/10.1158/0008-5472.CAN-15-3125.
22 Mayes K, Elsayed Z, Alhazmi A, et al. BPTF inhibits NK cell activity and the abundance of natural cytotoxicity receptor co-ligands. *Oncotarget*. 2017;8(38):64344–64357.
23 Urick AK, Hawk LML, Cassel MK, et al. Dual screening of BPTF and Brd4 using protein-observed fluorine NMR uncovers new bromodomain probe molecules. *ACS Chem Biol*. 2015;10(10):2246–2256. https://doi.org/10.1021/acschembio.5b00483.
24 Zhang D, Han J, Lu W, et al. Discovery of alkoxy benzamide derivatives as novel BPTF bromodomain inhibitors via structure-based virtual screening. *Bioorg Chem*. 2019;86:494–500. https://doi.org/10.1016/j.bioorg.2019.01.035.
25 Xu J, Wang Q, Leung ELH, et al. Compound C620–0696, a new potent inhibitor targeting BPTF, the chromatin-remodeling factor in non-small-cell lung cancer. *Front Med*. 2020;14(1):60–67. https://doi.org/10.1007/s11684-019-0694-8.
26 TP-238 https://www.thesgc.org/chemical-probes/TP-238 (accessed 2021 -03 -29).
27 NVS-BPTF-1 https://www.thesgc.org/chemical-probes/NVS-BPTF-1 (accessed 2021 -03 -12).
28 Xiong L, Mao X, Guo Y, et al. Discovery of selective BPTF bromodomain inhibitors by screening and structure-based optimization. *Biochem Biophys Res Commun*. 2021;545:125–131. https://doi.org/10.1016/j.bbrc.2021.01.067.
29 Kirberger SE, Ycas PD, Johnson JA, et al. Selectivity, ligand deconstruction, and cellular activity analysis of a BPTF bromodomain inhibitor. *Org. Biomol. Chem.* 2019;17(7):2020–2027. https://doi.org/10.1039/C8OB02599A.
30 Zhao X, Zheng F, Li Y, et al. BPTF promotes hepatocellular carcinoma growth by modulating HTERT signaling and cancer stem cell traits. *Redox Biol*. 2019;20:427–441. https://doi.org/10.1016/j.redox.2018.10.018.
31 Green AL, DeSisto J, Flannery P, et al. bptf regulates growth of adult and pediatric high-grade glioma through the MYC pathway. *Oncogene*. 2020;39(11):2305–2327. https://doi.org/10.1038/s41388-019-1125-7.
32 Heink S, Ludwig D, Kloetzel P-M, Krüger E. IFN-γ-induced immune adaptation of the proteasome system is an accelerated and transient response. *PNAS*. 2005;102(26):9241–9246. https://doi.org/10.1073/pnas.0501711102.